



Surface characterization of natural and Ca-saturated soil humic-clay composites at the micrometer scale: Effect of Calcium

Sofia Oufqir^{(1,2)*}, Paul R. Bloom⁽²⁾, Brandy M. Toner⁽²⁾, Mohammed EL Azzouzi⁽¹⁾

⁽¹⁾ Laboratoire des Matériaux, Nanotechnologies et Environnement, Département de Chimie, Faculté des sciences, Université Mohammed V-Agdal. BP 1014-Avenue Ibn Battouta. Rabat-Maroc

⁽²⁾ Department of Soil, Water, and Climate, University of Minnesota. Saint Paul, MN, 55108, MN, USA

Received 17Feb 2015, Revised 01 May 2015, Accepted 02 May 2015

*Corresponding author: E-mail: oufqi001@umn.edu

Abstract

Calcium is a pivotal element in the interactions between humic material and clay minerals favoring the stabilization of the formed micro-aggregates. Yet, morphological and structural knowledge of the humic-clay mineral surface is limited. In the present paper we employed the scanning electron microscopy (SEM) as a potent tool to analyze the surface texture of a humic-clay composite (HCC) fractionated from a prairie field soil and of a calcium saturated humic-clay composite (HCC-Ca) of the same soil. We aim to discern the influence of the addition of calcium ions on the surface of interaction. We applied statistical analyses to quantitatively characterize the morphology and the structure of the surface of the prepared samples. The SEM image treatment analyses revealed significant differences in the morphological structure and grains distribution in the HCC sample compared to the HCC-Ca sample. From our findings, we conclude that the presence of calcium in micro-soil plays a big role (i) in enlarging the size of the grains composing the surface of the humic-clay fraction by binding the mobile micro-particles, (ii) in readjusting the surface in a manner to homogenize the rough and random distribution of the humic-clay grains on the mineral surface, (iii) and in thickening the clay mineral layers promoting a better uptake of the humic material. This study disseminates a neat explanation of how calcium ions contribute in the stabilization of humic-clay aggregates in soil, and hence in the stabilization of carbon in the global carbon cycle.

Keywords: Humic-clay composite, Stabilization, Aggregates, Calcium, Surface structure, SEM

1. Introduction

The aggregation of the smectite-rich aluminosilicate clay mineral particles with humic substances is crucial for the stability of soils, and for the cycling of carbon. These associations are very important because of their ability to sustain soil fertility, and increase agricultural crop yields. The presence of calcium ions largely enhances humic sorption on clay particles. It is thought that calcium alters the structure of humic substances and mineral surfaces promoting the stabilization of their formed micro-aggregates and of the structure and texture of soil. However this knowledge is limited. Structural microscopic characterization of the humic-clay surface is needed for a better understanding of how calcium impacts this association. Literature states that the stabilization of humic material depends strictly on soil texture and clay mineralogy [1-5]. On the other hand, calcium constitutes a critical element affecting this stabilization [6-10] by causing huge alterations in the physical make up of the humic molecules [11, 12]. The focus has been only on determining the impact of calcium on the adsorption of organic matter onto clay surfaces using especially wet chemistry techniques, and on studying the molecular weights of humic material. The drawback of wet chemistry is that it does not reflect the real conditions available in the real environment. We need to visually discern the structural characterization of the humic-clay surface, and explain the effect calcium executes on the interaction surface that has yet not been investigated. To fulfill this gap, we chose to conduct microscopic analysis of the surface structure and morphology using the scanning electron microscopy tool. The purpose of our work was to evaluate the surface of association between humic

materials and clay minerals and to assess the effect of calcium ions on this association by studying the different features of the humic-clay compounds using microscopic technique. We aimed to (1) analyze the chemistry and visualize the surface structure of a humic-mineral composite based on SEM images, (2) investigate the impact of the calcium ions on the formation of the micro-aggregates, (3) statistically quantify the different characteristics caused by calcium ions. We hypothesize that calcium alters the surface of the humic-clay composite and contributes in the production of wide-size aggregates.

2. Materials and Methods

2.1. Preparation of humic-clay samples

We collected a soil from the surface (0-15cm of depth) of a prairie located in the South-West of Minnesota, USA. The soil was first mixed, air-dried, and then passed through a stainless steel 2.0 mm sieve to remove unwanted debris. Subsequently, we applied particle size fractionation to separate the soil clay fraction containing humic-clay composites from the soil by sedimentation. 25 grams of 2-mm sieved soil were dispersed in de-ionized water, all placed into 250ml centrifuge bottle, by shaking overnight at medium speed; then were decanted according to Stokes Law. The upper suspension was siphoned after the appropriate settling time. The whole process was repeated exhaustively until recovery of the quasi majority of all $<2\mu\text{m}$ fraction from soil. The collected humic-clay fraction was dewatered by centrifugation at 13,000rpm for 20min, and then freeze-dried. A total of ~ 500g of soil was used to eventually produce a quantity of ~ 83g of $<2\mu\text{m}$ humic-clay sample. A 40grams portion of the prepared sample was saturated with calcium ions by washing four times with 1 M CaCl_2 , followed by a dialysis against de-ionized water until removal of chlorine ions, then freeze-dried prior to analysis. The mineralogical composition of the prepared samples was determined using X-ray powder diffraction model PANalytical's X'Pert PRO MPD. The X-ray diffractometer is equipped with a copper rotating anode and a monochromator to select the $\text{Cu-K}\alpha$ radiation of a wavelength equal to 1.54 Å. The samples were mounted as pellets and the analysis was performed at the UATRS-CNRST center in Rabat, Morocco. The mineralogical phase was identified by fingerprint matching of the experimental powders.

2.2. Scanning Electron Microscopy analysis

The surface topography and the morphological and analytical characterization and examination of aggregates were performed at an electronic scale using a scanning electron microscope type environmental (brand FEI Quanta 200). The equipment is coupled to a system of x-ray microanalysis providing the chemical composition of the studied samples. The low frequency detector (LFD) was used for the topographic images, and the SUTW-Sapphire detector for the energy dispersion x-ray analysis (EDXA). The measurements of the HCC and HCC-Ca samples were carried out at high resolution and low vacuum mode (0.1 mbar-1.33 mbar), at an accelerating voltage of 16 kV, and at three different magnifications, low 5,000 \times , medium 10,000 \times , and high 20,000 \times , but we only present data at low and high magnifications. The work distance range was of 9.2-9.6 mm. The statistical analyses presented in this paper along with the structural analyses of the surface and the image treatments of the studied samples were generated and accomplished by certain tools provided by the sophisticated Mountains Map software, version Premium 7.1.

3. Results and discussions

3.1. SEM imaging - Elemental analysis

SEM topographic images of the humic-clay samples, HCC and HCC-Ca, were measured at three different magnifications with (x,y) image lengths corresponding to (55.6, 47.9) μm and (13.9, 12.0) μm at low and high magnifications respectively (Figure.1a and 1c). The images were filtered to remove noise, and then optimized for a better quality resolution. It is noticeable from the appearance of the images, at the entire magnification range, that the samples exhibited a variation in the shape and the size of the surface features as well as in the distribution of particles, which clearly outlines the impact of calcium ions on the humic-clay interactions. The XRD measurements were carried out to identify the major mineral phase composing the studied humic-clay composites. The analysis resulted in smectite being the dominated clay mineral with abundance of quartz nanoparticles; data are not shown in this paper. The EDX data revealed in general an approximately comparable chemical composition, but the decrease in sodium and magnesium content suggested their exchange with calcium ions (Table.1). On the other hand, we observed that the Al/Fe, Si/Al, and Si/Fe ratios corresponding to

the main aluminosilicate elements were not affected by the addition of calcium ions, they remained relatively unchanged. Al/Fe ratio had a value equal to 1.77 in HCC and 1.76 in HCC-Ca, whereas the values of Si/Al and Si/Fe slightly varied from 2.80 and 4.96 in HCC to 2.64 and 4.67 in HCC-Ca respectively.

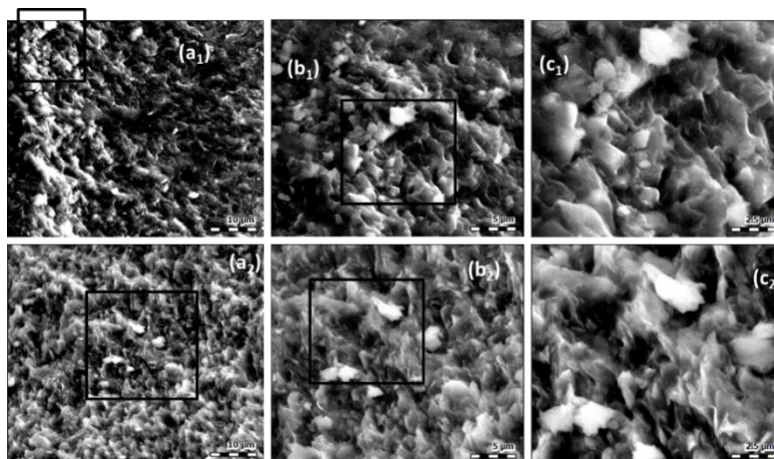


Figure 1: SEM images of the humic-clay composite HCC (a₁, b₁, and c₁) and the calcium saturated humic-clay composite HCC-Ca (a₂, b₂, and c₂) at low magnification 5,000× (a₁, a₂), medium magnification 10,000 (b₁, b₂), and high magnification 20,000× (c₁, c₂).

In short, except for the cation exchange, the observed relationship between the different elements contained in our samples along with XRD results pointed out that calcium ions might have a noteworthy effect on the surface texture and on the rearrangement of the humic-clay elements rather than on the chemical composition. Therefore, to further our understanding on this topic advanced imaging analysis and structural characterization of the interaction surface is necessary.

Table 1: Elemental composition of the natural humic-clay composite (HCC) and the calcium saturated humic-clay composite (HCC-Ca) measured using the energy dispersion X-rays coupled to the scanning electron microscope.

Element	Weight %		Atomic %	
	HCC	HCC-Ca	HCC	HCC-Ca
C	27.54	21.77	38.46	31.74
O	42.8	44.22	44.88	48.4
Na	0.15	0.27	0.11	0.21
Mg	0.96	1.01	0.67	0.73
Al	6.15	7.25	3.82	4.71
Si	17.24	19.2	10.3	11.97
K	1.06	0.96	0.45	0.43
Ca	0.63	1.2	0.26	0.52
Fe	3.47	4.11	1.04	1.29
Total	100	100	100	100

3.2. Grains Statistics

The analysis of the grains forming the surface of the humic-clay samples is essential to quantitatively identify the particle sizes and the morphology of the interaction surface. Moreover, this evaluation would allow us to define the behavior calcium exhibits towards the particle aggregates. Figure 2 illustrates grain topography and grain structure of micro-aggregates in HCC and HCC-Ca samples captured at high magnification. We observed

a remarkable decrease in the number of grain particles when calcium ions were added. This might be explained by aggregation of the humic-clay surface particles through calcium binding. The results of the generated statistical analysis of all grains are shown in Table 2. At low magnification and within approximately the same occupied area, HCC sample featured 10,620 grains on the surface with a density of 3.99 grains/ μm^2 , whereas HCC-Ca featured only 1,581 grains with a density of 0.632grains/ μm^2 . Similarly, at high magnification, the number of grains dropped from 27,763 to 15,789 with a density of 167 grains/ μm^2 in HCC but 94.9 in HCC-Ca grains/ μm^2 . On the other hand, the mean diameter parameter increased considerably from 31.7nm to 99.6nm and from 3.80nm to 4.16nm at low and high magnifications respectively, which suggest the enlargement of surface grains in the presence of calcium ions. However, the very high values of the derived standard deviation, especially at low magnification, denote a great dispersion of the data, which is attributed to a large variability in grains diameter. These high values might indicate lack of reliability when using the mean values for quantifying the grains diameter. In Figure 3, it is shown that effectively there is a prominent diversity of grains in size and shape. And this was more evident when we separated the extra-large grains from the small ones and had a general view of all grains constituting the surface of each sample. But it is also demonstrated from the images depicting the small sized grains (Figure 3c and 3f) that HCC-Ca exhibited wider surface particles compared to HCC particles. Moreover, the significant standard deviation values of the compactness parameter obtained at high magnification confirm the reliability of our findings. Therefore, the variation observed within the grains diameter, can be explained by the existence of large sized grains but simultaneously abundance of small to tiny particles within each sample.

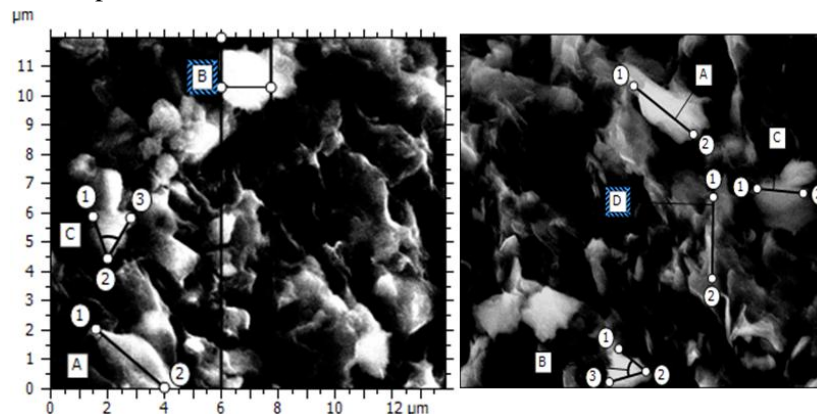


Figure 2: SEM topography of micro-aggregates in HCC (a) and HCC-Ca (b) samples, captured at high magnification (20,000 \times), showing grain content and grain particle-size.

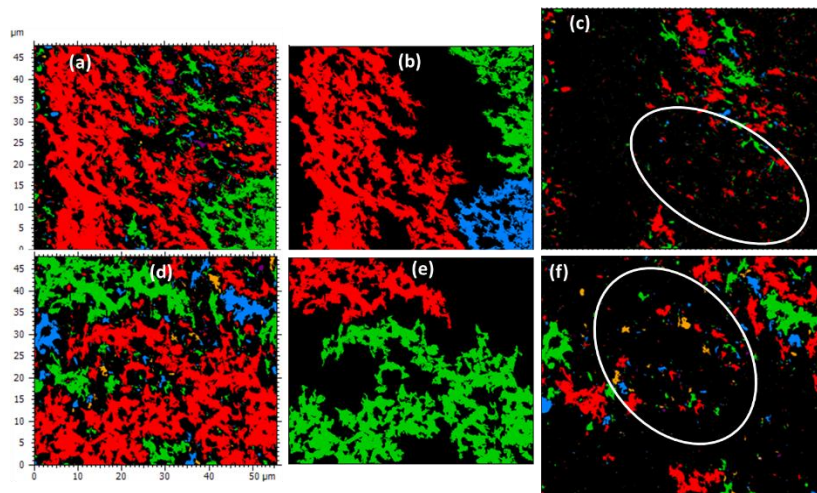


Figure 3: Analysis of all grains contained in HCC (a) and HCC-Ca (d) samples at high 20,000 \times magnification, the grains above the threshold of 50% (b, e), and the grains below the threshold (c, f) showing enlargement of particles in the calcium saturated humic-clay composite HCC-Ca

The drastic reductions in the number of grains, along with the increase in the diameter ascertain the role calcium plays in the aggregation of surface particles, and confirm our hypothesis. Calcium seemed to be involved in the enlargement of surface particles probably through cation binding which is in good agreement with the findings of [8, 13] and [14]. To investigate the observed differences in surface particles, a detailed analysis and characterization of the surface structure is needed.

3.3. Structural analysis

In order to proceed to the structural analysis, we first converted the SEM images of the HCC and HCC-Ca samples into surfaces as shown in figure 4a. We observed that humic-clay particles are spread out evenly on the surface of the HCC-Ca but are aggregated unequally on the surface of the HCC sample at low magnification. On the other hand, we analyzed the surface using the Fourier transform to determine the isotropy of the samples and the dominant directions on a polar plot (Figure 4b)..

Table 2: Generated statistical analysis of all grains contained on the surface of HCC and HCC-Ca samples at low (5,000×) and high (20,000×) magnifications by Mountains Map software. The grain parameters are presented as mean values; and Std. dev. abbreviation stands for standard deviation.

	Low Magnification				High Magnification			
	HCC		HCC-Ca		HCC		HCC-Ca	
Number of grains	10620		1681		27763		15789	
Total area occupied by grains	1236 μm ² (46.4%)		1208 μm ² (45.4%)		76.8 μm ² (46.1%)		78.0 μm ² (46.9%)	
Density of grains	3.99 Grains/μm ²		0.632 Grains/μm ²		167 Grains/μm ²		94.9 Grains/μm ²	
Grain parameters	Mean	Stddev	Mean	Stddev	Mean	Stddev	Mean	Stddev
Mean diameter, nm	31.7	87.8	99.6	262	3.8	14.8	4.16	26.1
Min Mean diameter, nm	19.6	48.2	56.3	135	2.8	7.75	3.02	15.4
Compactness	0.746	1.24	0.77	0.913	0.755	0.365	0.759	0.361

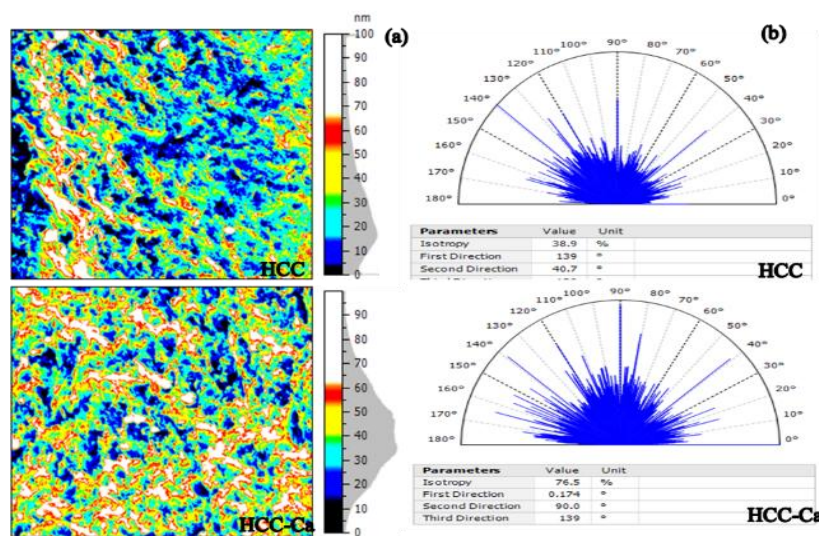


Figure 4:(a)Surface microstructure of the humic-clay composite HCC and the calcium saturated humic-clay composite HCC-Ca measured at low magnification (5,000×). (b) Polar plot of texture direction and isotropy of the HCC and HCC-Ca samples

The results revealed inequality in the texture direction between the two samples. HCC sample seemed to have an oriented texture with an isotropy of 38.9% contrarily to HCC-Ca that had a higher isotropy percentage of

76.5 indicating that the surface resembles itself in most of the surface directions. The dominant layer directions of the HCC surface were 139 degree for the first direction, 40.7 degree for the second direction, and 128 degree for the third one compared to 0.174, 90, and 139 degrees in HCC-Ca surface respectively. Therefore, we can say that the morphology and the texture direction of the humic-clay surfaces are likely determined based on the nature of ions present in the composite. Here we proposed to deeply explore the structure of our samples by detecting and visualizing the particles and bumps as well as the furrows composing the surface of the humic-clay minerals.

3.3.1. Islands

In this part of analysis, we detected a variety of islands (grains, particles, bumps) contained above the threshold heights we selected (50nm) on HCC and HCC-Ca surfaces (Figure 5). We found that the islands in HCC-Ca surface are dispersed all over the studied area coherently contrarily to HCC surface that has particles with elevated height located in one area on the mineral. This might indicate that calcium ions help in homogenizing the distribution of particles on the mineral surfaces. Statistics and data were generated for all islands (Table 3). At a threshold height of 50nm, HCC sample exhibited 665 and 332 islands, whereas HCC-Ca showed only 609 and 191 islands at low and high magnifications respectively. These numbers confirm the previously seen impact of calcium in producing large size aggregates and particles. The morphological parameters listed in table 4 show that HCC islands are characterized by a mean area of 0.564 and 0.144 μm^2 , a mean perimeter of 2764 and 1055nm, a mean diameter of 337 and 87,3nm, and a mean volume of 10,590,987 and 2,837,874 nm^3 at high and low magnifications respectively.

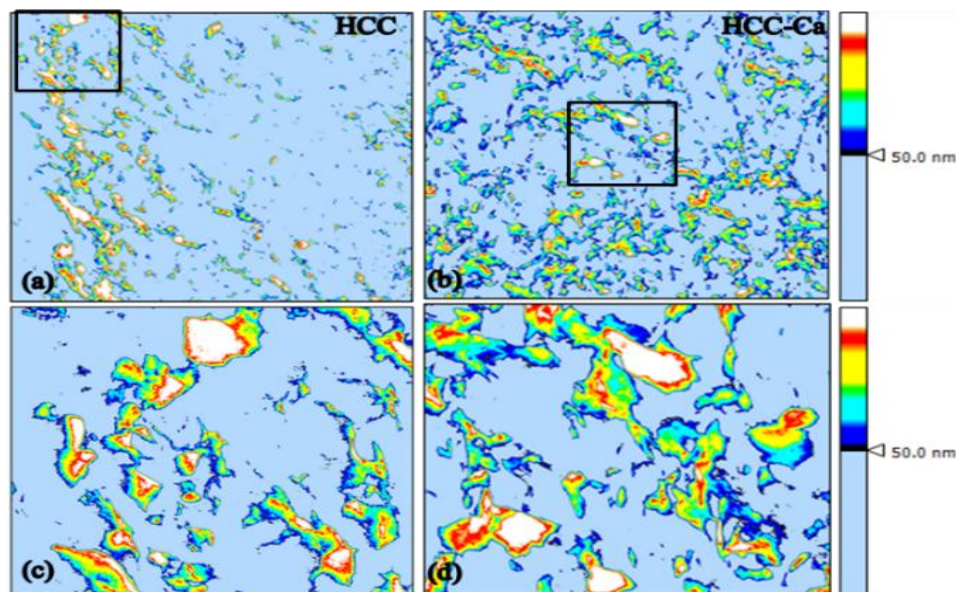


Figure 5: Islands detected above the threshold height of 50nm on HCC (a, c) and HCC-Ca (b, d) surfaces at 5,000 \times magnification (a, b) and 20,000 \times magnification (c, d).

While the HCC-Ca islands are characterized by a mean area of 1.28 and 0.332 μm^2 , a mean perimeter of 4659 and 1821 nm, a mean diameter of 403 and 143 nm, and a mean volume of 16,071,751 and 6,000,101 nm^3 at high and low magnifications respectively. The mean height/surface ratio constitutes an interesting parameter in the characterization of the surface structure as well. We observed a significant decrease from 249 to 130 $\text{nm}/\mu\text{m}^2$ at low magnification, and from 2622 to 1444 $\text{nm}/\mu\text{m}^2$ at high magnification suggesting that the homogeneity of the HCC-Ca surface compared to HCC surface. Briefly, we infer then that calcium ions are involved in restructuring the interaction surface by affecting the distribution of surface particles, and modifying the surface morphology and texture in a manner to promote the formation of larger aggregates.

Table 3: Calculates statistics and data of all islands figuring on HCC and HCC-Ca samples. Selected mean islands parameters are listed as mean values at low (5,000×) and high (20,000×) magnifications.

Sample	Low Magnification		High Magnification	
	HCC	HCC-Ca	HCC	HCC-Ca
Number of Islands	665	609	332	191
Threshold	50	50	50	50
Islands parameters, Mean				
Area, μm^2	0.564	1.28	0.144	0.332
Perimeter, nm	2764	4659	1055	1821
Mean diameter, nm	337	403	87.3	143
Min diameter, nm	197	227	50.9	86.4
Max diameter, nm	638	767	161	263
Volume, nm^3	10590987	16071751	2837874	6000101
Height/Surface ratio, $\text{nm}/\mu\text{m}^2$	249	130	2622	1444

3.3.2. *Furrows*

The second part of the structural analysis consisted in visualizing surface furrows above and below a threshold height of 50%, and in calculating furrow parameters that are maximum depth, mean depth and mean density. Figure 6 displays all the resulted furrows (Figure6a), the furrows below the specified threshold height (Figure6b), and the furrows above a threshold height (Figure6c). In fact, we compared the surface network before and after saturation with calcium cations at low magnification, the furrow parameters revealed a strong decrease in mean density of about 46% (from 23919 to 13821 cm/cm^2) after saturation with calcium ions. The mean depth decreased from 42.7nm with a maximum of 92.5nm to 29.4nm with a maximum of 67.9nm. We separated the main and secondary furrows at the threshold of 50% in the purpose to carefully visualize the surface structure. The mean density of furrows deeper than the threshold was about two times bigger in HCC sample than in HCC-Ca sample, while the mean depth was 55.7 for HCC versus 43.2nm for HCC-Ca. The mean density of furrows above threshold was 13074 cm/cm^3

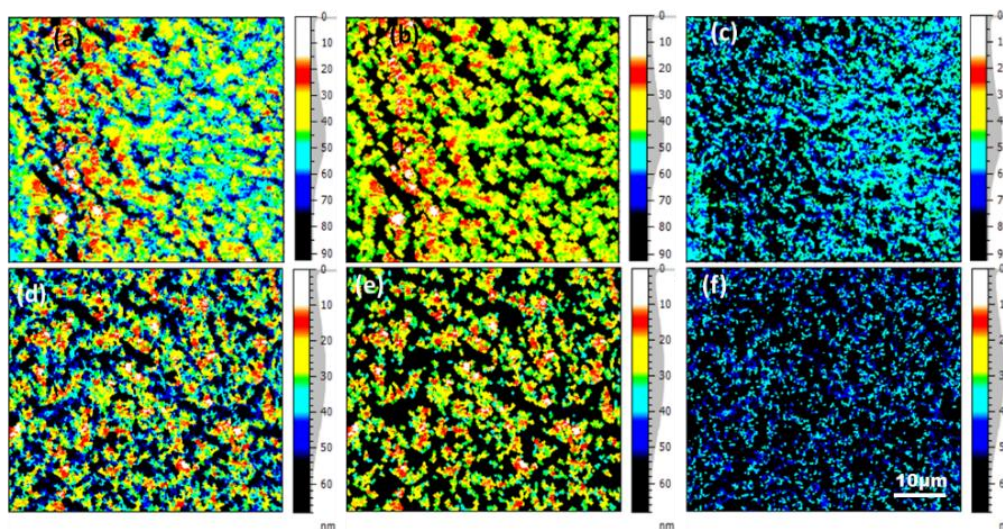


Figure6: visualization of all surface furrows (a, d), the furrows below the threshold height of 50% (c, f), and the furrows above a threshold height (b, e) for HCC (a, b, c) and HCC-Ca (d, e, f) samples at low (5,000×) magnification.

in HCC sample but 8030 cm/cm³ in HCC-Ca sample, while the mean depth was 32.3nm for HCC with a maximum of 46.3nm versus 20.3nm for HCC-Ca with a maximum of 34nm. We found similar results at high magnification. So the observed decrease in the depth and the density on HCC surface indicates that calcium ions smoothen the surface and regulate the distribution of surface particles to approximately equal thicknesses, which confirms the inferences drawn from grains analyses. We infer from here the positive effect calcium has in the mobility of nutrients and metals in soil, in the aeration of soil, and in retaining water in soil which is in great favor of crops and agriculture.

3.4. Functional analysis

Another relevant aspect of the analytical approach adopted in this paper was the assessment of the interaction surface functionality. The following part of study deals with the basic surface texture analysis including mainly thickness of three horizontal slices and bearing ratio curve as well as depth distribution histogram.

3.4.1. Slices

We considered to study the volume and thickness of the material laid all over the generated planes. As a matter of fact, the analysis consisted in slicing the surface at the 25nm and 75nm thresholds out of a 100nm scale to eventually produce three different slices of varied particle depth. Figure 7 depicts the resulting slices for the two studied samples at low and high magnifications. We found at low magnification that the majority of the material composing the humic-clay sample HCC has a height lower or equal to 25.1nm, and occupies 50.4% of the projected area of which 77.3% is the volume of material and 22.7% is the volume of void. The second slice, of height comprised between 25.1 and 74.9 nm, represents 45% of the projected area with only 18.7% corresponding to the volume of material but 81.3% of void volume. The third slice representing material with height higher than 74.9nm is very limited in projected area, only 4.17% of which 2.13% is material. As for HCC-Ca sample, we found instead that the high majority of the total surface area (82.1%) is abundantly covered with particles having a height range of 25-27nm and a volume of material of 36.7%. Only 14.9% of the area has particles with height lower than 25nm but occupy 96% of it. We observed the same trend of results at high magnification. It is elucidated then that calcium ions might be responsible of the differences in the distribution of surface particles. On the other hand, we compared the mean thickness of surface particles in both samples and we noticed that even though the HCC contained much more material in the first slice, its corresponding mean thickness was much smaller than that of HCC-Ca which may be explained by the swelling potential of calcium ions. Calcium uniforms the distribution of particles on the mineral surface and increases the surface thickness.

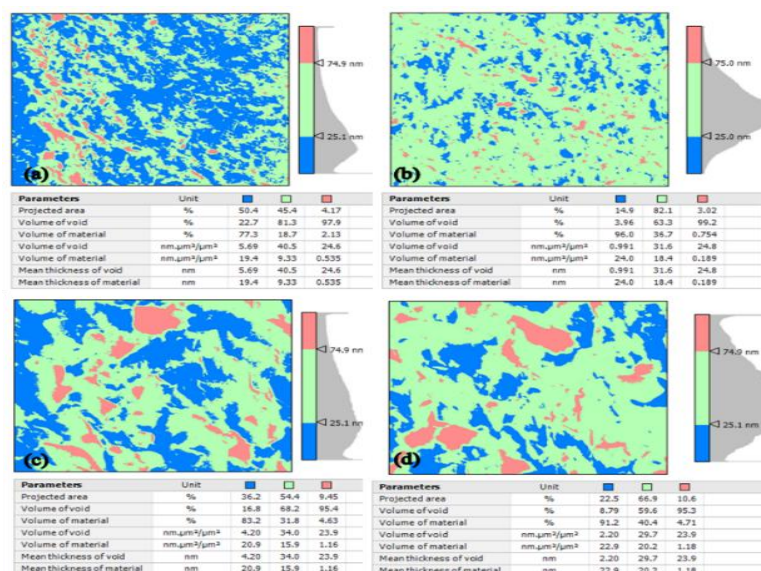


Figure 7: Surface slices of varied particle depth at 25nm and 75nm thresholds of HCC (a, c) and HCC-Ca (b, d) samples at 5,000 \times magnification (a, b) and 20,000 \times magnification (c, d).

3.4.2. Abbott-firestone curve

The Abbott Firestone Curves are important in surface characterization. They present the amount of material present at selected heights of the surface profile. Its statistical character allows the observation of the profile amplitude representing the depth distribution. In this study we used the Abbott-Firestone curve to describe the surface texture of the HCC and compare it to that of the HCC-Ca to evaluate the impact of calcium by different means to evidence the consistency of our findings.

The Figure 8 shows the depth distribution of the data points on the studied surfaces. We found that 12.1% of the HCC surface points represent the largest population with a depth range of 75-80.5nm, while there is only 11.5% for HCC-Ca are with a range of 60.5-65.0nm. On the other hand, the section height between 5% and 95% of material ratio is 71.4 nm for HCC sample against 53.9 nm after saturation with Ca ions. These results confirm that the presence of calcium ions help in readjusting the surface structure in a manner to re-aggregate the rough surface components. The calcium flattens the surface by curtailing the height of the micro-particles. Moreover, it homogenizes to some extent the mineral surface which is demonstrated through the normality of the statistical distribution of the surface points.

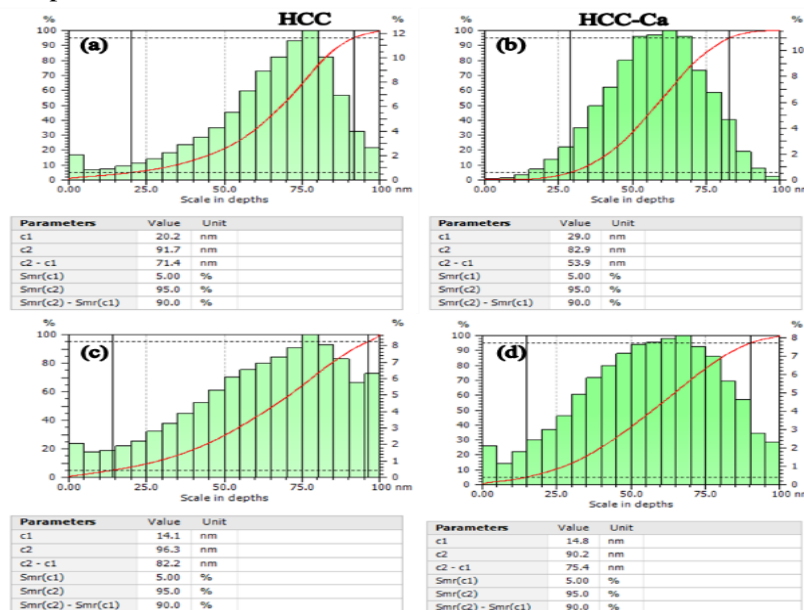


Figure 8: Abbott Firestone Curves of HCC (a, c) and HCC-Ca (b, d) samples at 5,000× magnification (a, b) and 20,000× magnification (c, d) showing the amount of material present at various heights of the surface profile.

Conclusion

In this study we evaluated the impact of calcium on the stabilization of humic-clay aggregates at a microscopic scale. We analyzed the chemical composition and surface structure of a humic-clay composite separated from a carbon rich-soil. Our findings and inferences suggest that the calcium ions contribute in the enlargement of the micro-aggregates composing the humic-clay mineral surfaces through binding of the mobile micro-particles. This morphological alteration in humic-clay aggregates promotes the stabilization and uptake of humic material fractions and carbon in soil and favors the retention of water as well. The calcium ions exhibited also a great effect in readjusting the surface structure in a manner to restructure the rough surface components. It homogenized to some extent the mineral surface, which is demonstrated through the statistical distribution of the surface points. Moreover, the present study showed the swelling capacity of calcium ions lying on the increase in thickness of the humic-clay minerals. The outcomes of this study would be of great help for calcium, humic-clays, and carbon stabilization studies.

Acknowledgements – This work was supported by the Ministry of higher education, scientific research and executive training of Morocco. We thank the national center for scientific and technical research of Morocco for the SEM measurements.

References

1. Deneff K., Six, J., Merckx R., Paustian K., *Soil Sci. Soc. Am. J.* 68 (2004) 1935.
2. Kaiser K., Guggenberger G., Haumaier L., Zech W., *Organic Geochem.* 33 (2002) 307.
3. Schulten H-R, Leinweber P., *Biol. Fertil. Soils.* 30 (2000) 399.
4. Baldock J.A., Skjemstad J.O., *Organic Geochem.* 31 (2000) 697.
5. Christensen B. T., *Adv. Soil Sci.* 20 (1992) 1.
6. Grant C.D., Dexter A.R., Oades J.M., *Soil Till. Res.* 22 (1992) 283.
7. Baldock J.A., AoyannaM., Oades J.M., Grant C.D., *Aust. J. Soil Res.* 32 (1994) 571.
8. Muneer M. &Oades J.M., *Aust. J. Soil Sci.* 27 (1989) 411.
9. Chan K.Y., Heenan D.P., *Aust. J. Soil Res.* 36 (1998) 73.
10. Chan K.Y., Heenan D.P., *Soil Sci. Soc. Am. J.* 63 (1999) 1841.
11. Kolla S., Humic Substances: Structures, Properties and Uses. *Royal Soc. Chem. Cambridge, UK.*(1998) 216.
12. Piccolo A., Conte P. and Cozzolino A., Humic Substances: Versatile Components of Plants, Soil and Water. *Royal Soc. Chem. Cambridge, UK.* (2004) 120.
13. Bronick C.J., Lal R., *Geoderma.* 124 (2005) 3.
14. Six J., Bossuyt H., Degryze S., Deneff K. *Soil Till Res.* 79 (2004) 7.

(2015); <http://www.jmaterenvirosci.com>